The microwave spectrum and structure of the H2O–SO2 complex

K. Matsumura, F. J. Lovas, and R. D. Suenram

Citation: The Journal of Chemical Physics **91**, 5887 (1989); doi: 10.1063/1.457457
View online: http://dx.doi.org/10.1063/1.457457
View Table of Contents: http://scitation.aip.org/content/aip/journal/jcp/91/10?ver=pdfcov
Published by the AIP Publishing

The microwave spectrum and structure of the H_2O–SO_2 complex

K. Matsumura,[a] F. J. Lovas, and R. D. Suenram
Molecular Spectroscopy Division, National Institute of Standards and Technology, Gaithersburg, Maryland 20899

(Received 16 March 1989; accepted 27 July 1989)

The microwave spectrum of H_2O–SO_2 has been observed with a pulsed beam, Fabry–Perot cavity, Fourier-transform microwave spectrometer. In addition to the normal isotopic form, we have observed the spectra of H_2O–$^{34}SO_2$, HDO–SO_2, and D_2O–SO_2. For the normal and dideuterated forms we observe two states with *a*- and *c*-type spectra which are split by internal rotation of the water unit, while for the ^{34}S and HDO species two states are observed but only the *a*-type spectrum was assigned. Rotational analysis of each spectrum for H_2O–SO_2 provides the constants $A = 8763.071(3)$ MHz, $B = 3819.655(2)$ MHz, and $C = 2900.899(2)$ MHz for the $I = 0$ state and $A = 8734.268(4)$ MHz, $B = 3821.281(2)$ MHz, and $C = 2900.837(2)$ MHz for the $I = 1$ state, where I is the resultant proton nuclear spin. Stark effect measurements give electric dipole components $\mu_a = 1.984(2)$ D and $\mu_c = 0.488(4)$ D for H_2O–SO_2. The geometry obtained from fitting the derived moments of inertia has the planes of the two monomer units tilted approximately 45° from the parallel orientation with the oxygen atom of the water closest to the S atom of SO_2, giving an S–O distance of 2.824(16) Å and a center-of-mass distance $R_{c.m.} = 2.962(5)$ Å. The $(SO_2)_2$ species was also produced with the same nozzle expansion conditions as used for H_2O–SO_2. New measurements on $(SO_2)_2$ are reported and fitted with the measurements from Nelson, Fraser and Klemperer [J. Chem. Phys. **83**, 945 (1985)], providing improved rotational and centrifugal distortion constants.

I. INTRODUCTION

A major atmospheric problem which has received growing attention in recent years is the formation of acid rain, principally from industrial emissions. The corrosive character of the atmospheric components has a detrimental effect on plants and wildlife, particularly those associated with an aquatic environment.[1-3] The term "acid rain" is generally used to describe precipitation that has a *p*H below 5.6. A *p*H value of 5.6 is attained by water in equilibrium with atmospheric CO_2.[4] The major chemical species responsible for acidification of rain water beyond this limit have been found to be H_2SO_4, HNO_3, and HCOOH. Qualitatively, these species are formed by the dissolution of acidic sulfate aerosols, nitric acid vapor, and the aqueous-phase oxidation of gaseous sulfur dioxide and formaldehyde.[2] However, the primary species implicated in the formation of acid rain is SO_2. Sulfur dioxide enters the atmosphere from anthropogenic sources such as the burning of fossil fuels and the smelting of sulfur-bearing ores. Once in the atmosphere, it can be transformed by a number of reaction pathways which eventually yield sulfuric acid as the product. While free sulfurous acid, H_2SO_3, is not known, it is present in aqueous solutions of sulfur dioxide, largely in the form of the HSO_3^- ion which may be oxidized by dissolved H_2O_2 or O_3 to form the sulfate ion. Several gas-phase oxidation reactions of SO_2 are thought to be important in producing SO_3 which forms H_2SO_4 upon dissolution.[1]

In an attempt to understand the complex chemical pathways related to the conversion of SO_2 to H_2SO_4 in the atmosphere, we have begun a study of the gas-phase complexes of SO_x species with other atmospheric components, such as H_2O, O_3, and H_2O_2. These complexes represent the initial step in the reaction path for dissolution and oxidation of the SO_x species. This paper reports the microwave spectrum and structure of the first of these, the H_2O–SO_2 complex.

II. EXPERIMENT

Spectral measurements were carried out with a Fabry–Perot cavity, Fourier-transform microwave spectrometer[5] with a heated pulsed-nozzle source.[6,7] A pulsed solenoid valve is used to deliver a supersonic molecular beam from a sample of about 1% SO_2 entrained in argon carrier gas at a total pressure of 120 Pa to the center of a Fabry–Perot cavity. Water was placed in the pulsed-valve reservoir which was heated to 40 °C to obtain optimum water monomer in the vapor phase. Beam pulses from a 0.5 mm orifice with 200–400 μs duration were employed with repetition rates up to 35 Hz. The molecular complex is polarized by a short microwave pulse when the microwave frequency is nearly resonant ($\Delta\nu \leqslant 0.5$ MHz) with a rotational transition of the complex. The free induction decay signal from the cavity is then digitized (512 points, 0.5 μs/point). Typically, 500–2000 pulses are signal averaged, after subtracting a background microwave pulse from each signal pulse, to yield good signal-to-noise ratios. The averaged data was Fourier transformed to obtain the power spectrum in the frequency domain with a resolution element of 3.9063 kHz/point. Molecular transitions have observed linewidths of 10^{-6} of the pump frequency, i.e., 10 kHz at 10 GHz, and the measure-

[a] Permanent address: Seinan Gakuin University, Nishijin, Sawaraku, Fukuoka 814, Japan.

 0021-9606/89/225887-08$02.10

ment precision and accuracy is estimated as 4 kHz, which is the resolution element.

The spectrum of $^{34}SO_2$–H_2O was observed with natural abundance ^{34}S, which is about 4% of the SO_2 in the sample. The dideuterated species was studied by placing 99% D_2O in the nozzle reservoir and the monodeuterated species was observed with a 50%–50% mixture of H_2O and D_2O in the reservoir.

III. SPECTRAL ANALYSIS

For van der Waals and hydrogen-bonded complexes of asymmetric top subunits, spectral predictions are difficult to make accurately since the structural conformation and interaction distances are quite uncertain. Often it is necessary to predict spectra for a number of chemically intuitive structures as a guide to the search range. Most of our structural estimates for the H_2O–SO_2 species, which ranged from O· ·H bonded forms to O· ·S van der Waals bonded structures, placed the a-type $J = 2$–1 transitions in the 10–16 GHz region. A spectral survey was initiated in the 10–12 GHz region; however, recognition of an a-type R-branch spectral pattern for a prolate rotor was hampered by the observation of rich spectra from other complexes. A majority of the transitions observed were eventually assigned to the $(SO_2)_2$ and Ar–SO_2 species whose spectra were identified in previous studies.[8,9] Since these prior analyses were insufficient for accurate prediction of the new spectral lines, we carried out new analyses of each. The identification of transitions from the Ar–SO_2 species was achieved by replacing the Ar carrier gas with Ne and observing that the transitions disappeared. The new measurements and analysis for Ar–SO_2 will be reported elsewhere,[10] while the new results for $(SO_2)_2$ are reported below.

A. Analysis of $(SO_2)_2$

In the previous study by Nelson, Fraser, and Klemperer,[8] most of the transitions measured were from states with $K_a \geqslant 2$, while in our measurements the strongest transitions arise from the $K_a = 0,1$ states due to the lower temperature of the pulsed beam (~ 1 K). The assignments were guided by predictions from a fit of the prior measurements. Only a-type transitions have been identified in both studies, and these are shifted by a small tunneling frequency (70 kHz) with the $K_a + K_c =$ even states being the lower-energy states. In the initial fits here, combination differences for the lower-energy state were calculated from transitions with a common upper-state level and then fitted to nine rotational and centrifugal distortion constants. These lower state constants were then fixed in a fit of all the transitions shown in Table I to obtain the ten upper-state constants shown in Table II. Since both upper- and lower-state constants were identical within their calculated standard deviations (except for the tunneling inversion frequency, Δ_{inv}), this latter fit was repeated by replacing the lower-state constants with the more accurate upper-state values to obtain the final values shown in Table II for both states. This analysis provides a much improved value for the A rotational constant and required two new parameters, Φ_{JK} and Φ_{KJ}, to fit the data

TABLE I. Rotational spectrum of $(SO_2)_2$.

Transition $J'_{K_aK_c}$–$J''_{K_aK_c}$	Frequency (MHz)	Obs. – Calc. (kHz)	Ref.
7_{34}–7_{35}	0.2490(20)[a]	1.8	8
3_{21}–3_{22}	1.3083(10)	– 0.7	8
5_{23}–5_{24}	8.7430(25)	– 1.1	8
7_{25}–7_{26}	31.2815(25)	– 1.1	8
9_{27}–9_{28}	81.700(7)	– 4	8
5_{14}–5_{15}	669.670(3)	0	8
7_{16}–7_{17}	1 249.842(5)	4	8
5_{41}–4_{40}	9 245.225(6)	1	8
5_{32}–4_{31}	9 252.488(6)	0	8
5_{05}–4_{04}	9 255.516(4)	0	
5_{23}–4_{22}	9 260.980(4)	0	
6_{16}–5_{15}	10 974.964(4)	0	
6_{43}–5_{42}	11 093.859(15)	– 1	8
6_{34}–5_{33}	11 102.715(11)	– 1	8
7_{43}–6_{42}	12 942.281(6)	1	8
7_{07}–6_{06}	12 949.332(4)	1	
7_{34}–6_{33}	12 952.936(20)	3	8
7_{25}–6_{24}	12 969.713(4)	– 1	
7_{16}–6_{15}	13 114.809(4)	0	
8_{18}–7_{17}	14 629.148(4)	2	
9_{09}–8_{08}	16 634.846(4)	– 1	
9_{18}–8_{17}	16 856.344(4)	1	
10_{29}–9_{28}	18 500.550(4)	– 2	
2_{21}–2_{20}	– 0.1747(13)	3.3	8
8_{36}–8_{35}	– 0.3245(60)	0.5	8
4_{23}–4_{22}	– 3.6483(20)	– 0.6	8
6_{25}–6_{24}	– 17.2758(23)	0.0	8
4_{14}–4_{13}	– 446.341(3)	0	8
6_{16}–6_{15}	– 937.3245(23)	0.2	8
4_{41}–5_{42}	– 9 245.088(9)	5	8
4_{32}–5_{33}	– 9 252.336(6)	– 3	8
4_{23}–5_{24}	– 9 255.884(4)	– 1	
5_{41}–6_{42}	– 11 093.724(35)	5	8
5_{32}–6_{33}	– 11 102.626(10)	0	8
5_{05}–6_{06}	– 11 103.176(4)	0	
5_{14}–6_{15}	– 11 242.620(4)	– 1	
6_{16}–7_{17}	– 12 802.296(4)	– 1	
6_{43}–7_{44}	– 12 942.151(3)	– 2	8
6_{34}–7_{35}	– 12 952.687(18)	2	8
6_{25}–7_{26}	– 12 955.707(4)	0	
7_{07}–8_{08}	– 14 793.128(4)	– 1	
7_{16}–8_{17}	– 14 985.907(4)	– 1	
8_{18}–9_{19}	– 16 454.848(4)	1	

[a] Measurement uncertainties in parentheses refer to the last digit(s) shown.

TABLE II. Spectroscopic constants of SO_2–SO_2.

Parameter	Present value	Ref. 8
A (MHz)	6922.8928(6)[a]	6958.5
B (MHz)	948.5328(4)	948.481
C (MHz)	903.7609(4)	903.839
δ_J (kHz)	0.0057(5)	· · ·
δ_K (kHz)	32.44(19)	· · ·
Δ_{JK} (kHz)	97.541 (27)	99.5
Δ_J (kHz)	2.1343(10)	2.17
Φ_{JK} (kHz)	– 0.041 04(37)	· · ·
Φ_{KJ} (kHz)	– 0.007 16(26)	· · ·
Δ_{inv} (kHz)	71.1(22)	70.(1)

[a] The uncertainty represents one standard deviation from the least-squares fit and refers to the last digit(s) shown.

TABLE III. Rotational spectrum of H_2O–SO_2 and D_2O–SO_2.[a]

	H_2O–SO_2				D_2O–SO_2			
State	A_1		A_2		A_1		A_2	
Spin wt.	1		3		6		3	
Transition $J'_{K_aK_c}$–$J''_{K_aK_c}$	ν (MHz)	$\Delta\nu^b$ (kHz)	ν (MHz)	$\Delta\nu^b$ (kHz)	ν (MHz)	$\Delta\nu^b$ (kHz)	ν (MHz)	$\Delta\nu^b$ (kHz)
4_{23}–4_{13}	...		11 761.997	1	...		...	
2_{12}–1_{11}	12 521.534	0	12 522.974	2	11 548.169	9	11 548.048	−2
1_{10}–0_{00}	12 582.052	−1	12 554.890	5	12 011.079	−6	12 006.452	9
2_{02}–1_{01}	13 324.364	−1	13 326.430	−1	12 252.210	5	12 252.163	−6
3_{22}–3_{12}	13 526.534	0	13 433.614	1	...		...	
2_{11}–1_{10}	14 357.496	1	14 362.304	−3	13 124.731	−2	13 124.996	−2
4_{13}–3_{21}	...		14 448.963	−1	...		...	
2_{21}–2_{11}	14 830.536	−2	14 739.398	−5	15 161.705	−3	15 147.165	1
2_{20}–2_{12}	17 700.786	1	17 615.774	1	17 611.750	1	17 597.874	−4
3_{13}–2_{12}	18 713.296	−2	18 714.861	0	17 271.190	2	17 270.954	−4
3_{21}–3_{13}	19 594.002	0	19 516.074	2	19 174.505	2	19 161.419	3
3_{03}–2_{02}	19 706.852	5	19 707.574	4	18 171.058	−3	18 170.752	6
3_{22}–2_{21}	20 153.502	1	20 158.180	−1	18 499.910	−3	18 500.037	−3
2_{11}–1_{01}	20 219.061	0	20 195.137	−5	18 966.995	7	18 962.565	−9
3_{21}–2_{20}	20 606.515	0	20 615.158	−2	18 833.937	5	18 834.505	9
3_{12}–2_{11}	21 457.502	−3	21 463.973	3	19 629.876	7	19 630.220	7
4_{14}–3_{13}	24 834.406	−2	24 835.576	−1	22 940.615	−2	22 940.205	1
4_{04}–3_{03}	25 812.975	2	25 810.748	0	23 874.534	2	23 873.730	1
4_{23}–3_{22}	...		...		24 599.295	3	23 599.390	0
4_{22}–3_{21}	...		...		25 396.263	2	25 397.303	−6

[a] Measurement uncertainty is estimated to be 4 kHz.
[b] Observed minus calculated frequency.

within experimental error. With predictions from this analysis we could account for all lines arising from the a-type spectrum of the $(SO_2)_2$ complex. A second selection rule is expected for $(SO_2)_2$, either *b*-type or *c*-type, but no transitions were identified at the frequencies predicted from the *a*-type transition fit. We have found several transitions in the 12–13 GHz region, whose chemical behavior indicates that they belong to this dimer, but they are too weak for Stark effect measurement. The tunneling splitting for the *b*- or *c*-type transitions must be considerably larger than for the *a*-type transitions, so assignments are more difficult.

B. Analysis of H_2O–SO_2

After accounting for the strong transitions of Ar-SO_2 and $(SO_2)_2$, the three $J = 2$–1 *a*-type transitions in the region from 12.5 to 14.4 GHz were located and assigned by Stark effect measurements. For each of these transitions a satellite line was observed with an intensity of about one-third of the stronger spectral line. The Stark effect was nearly identical for both components. The measurements were extended to higher J and K values which allowed us to predict and locate the *c*-type transitions which were found to be about a factor of 20 weaker than the *a*-type transitions. The measurements are listed in Table III along with the residuals from the fitting. A similar doublet spectrum was observed for the $^{34}SO_2$, HDO, and D_2O isotopic species. In the case of D_2O–SO_2 the intensity ratio of transitions from the two states was about 2/1, compared to 3/1 for the H_2O–SO_2 and H_2O–$^{34}SO_2$ species. The measurements for D_2O–SO_2 are given in Table III, those for H_2O–$^{34}SO_2$ are presented in Table IV and measurements for HDO–SO_2 are given in Table V.

Once the assignments were verified with Stark effect measurements, fitting the spectra to the I^r A-reduced Watson[11] centrifugal distortion Hamiltonian was straightforward for all but the HDO–SO_2 species. The molecular constants determined for H_2O–SO_2 and D_2O–SO_2 are listed in Table VI and those for the ^{34}S species are given in Table VII. The occurrence of two states appears to originate from a 180° internal rotation of the water unit about its C_2 axis, which interchanges the two equivalent hydrogens.

TABLE IV. Rotational spectrum of H_2O–$^{34}SO_2$.[a]

	H_2O–$^{34}SO_2$			
State	A_1		A_2	
Spin wt.	1		3	
Transition $J'_{K_aK_c}$–$J''_{K_aK_c}$	ν (MHz)	$\Delta\nu^b$ (kHz)	ν (MHz)	$\Delta\nu^b$ (kHz)
2_{12}–1_{11}	12 463.461	−1	12 464.929	3
2_{02}–1_{01}	13 254.359	0	13 256.450	0
2_{11}–1_{10}	14 268.757	1	14 273.528	−4
3_{13}–2_{12}	18 628.161	1	18 629.786	−2
3_{03}–2_{02}	19 609.759	0	19 610.594	0
3_{12}–2_{11}	21 326.755	−1	21 333.209	3

[a] Measured uncertainty is 4 kHz.
[b] Observed minus calculated frequency.

TABLE V. Rotational spectrum of HDO–SO_2.[a]

Transition $J'_{K_aK_c}$–$J''_{K_aK_c}$	Lower freq. ν_L (MHz)	$\Delta\nu$[c] (MHz)	Upper freq.[b] ν_U (MHz)	Difference $\nu_U - \nu_L$ (MHz)
2_{12}–1_{11}	12 012.508[d]	− 6.016	12 110.771	98.3
2_{02}–1_{01}	12 765.879	− 0.025	13 096.685	330.8
2_{11}–1_{10}	13 705.086	− 0.007	13 704.641	− 0.5
3_{13}–2_{12}	17 935.038[d]	− 32.866	18 210.530	275.5
3_{03}–2_{02}	18 910.272	0.031	19 087.130	176.9
3_{22}–2_{21}	19 280.393	− 0.001	19 295.552	15.2
3_{21}–2_{20}	19 665.972	0.001	19 674.407	8.4
3_{12}–2_{11}	20 489.991	0.004	20 517.960	28.0
4_{14}–3_{13}	23 851.160[d]	− 3.855	23 878.948	27.8
4_{04}–3_{03}	24 811.360	− 0.011	24 915.518	104.2
4_{23}–3_{22}	25 631.956[d]	6.558	25 651.891	19.9

[a] Measurement uncertainty is 4 kHz.
[b] This state was not fit.
[c] Observed minus calculated frequency.
[d] Not included in fit.

In light of the structure of H_2O–SO_2, discussed in Sec. IV, four equivalent frameworks can be produced from a 180° rotation of each monomer unit about its C_2 axis or from a geared inversion of the two units through a planar C_{2v} intermediate configuration. This situation is analogous to the feasible tunneling motions of H_2O–D_2O for which the rotation–vibration levels are A_1, A_2, B_1, and B_2 symmetry species.[12] Exchange of the spin-1/2 protons and spin-0 oxygen atoms in H_2O–SO_2 gives spin weights $g = 1, 3, 0, 0$ for the A_1, A_2, B_1, and B_2 states, respectively, and for D_2O–SO_2 the corresponding spin weights are $g = 6, 3, 0, 0$. Only two states occur with nonzero spin weight, as has been observed, and the state labels in Tables III, IV, VI, and VII were obtained from the observed relative intensities. A 180° rotation of the water (or SO_2) unit about its C_2 axis does not invert the dipole components, while a geared inversion of both monomer units would invert the μ_c dipole component and cause the c-type transitions to be split from the rigid rotor positions. The lack of additional tunneling splitting in the c-type transitions indicates that the geared inversion tunneling motion does not occur in this case. Since the spectra from the two observed states can be fit within experimental error with a Hamiltonian which does not include explicit tunneling terms, there is no indication that both monomer units are internally rotating. Because H_2O has the smallest moment of inertia, it is most likely that it is the source of the observed splittings. In fact, if only a 180° rotation of H_2O were occurring, the same result as described above for state labels and spin weights would be obtained.

For the HDO–SO_2 species, the internal rotation of HDO would also give spectra from two states, but no spin weight difference would occur. The observed splittings for various a-type transitions of HDO–SO_2 range from less than 1 MHz to more than 300 MHz, compared to only a few MHz for the transitions of the other isotopic species, and the weak c-type transitions were not identified. We have been unsuccessful in fitting either set of transitions to the measurement accuracy and conclude that the two states are perturbing one another through accidental near degeneracies. Only one of the spectra could be fit with modest success and the effective constants are shown in Table VII.

The electric dipole moments of three of the water-sulfur dioxide dimer isotopic species were determined by measurement of the frequency shift of the Stark components as a function of applied electric field. The electric field is obtained by applying equal positive and negative voltages to the parallel plates spaced at about 26 cm, and $\Delta M_J = 0$ selection rules were selected by orienting the E vector of the microwave field parallel with the applied field, as described previously.[7] Five Stark components of the A_1 and A_2 states of H_2O–SO_2 were measured with frequency shifts up to about 1 MHz for the highest electric field. These were the $|M_J| = 0, 1$ components of the 2_{02}–1_{01} and 2_{11}–1_{10} transitions and the $M_J = 0$ component of the 1_{10}–0_{00} c-type transition. A least-squares fit of 21 measurements yielded $\mu_a = 1.984(2)$ D and $\mu_c = 0.488(4)$ D for the A_1 state with nearly identical values obtained for the A_2 state as shown in Table VI. Measurements on the fitted state of HDO–SO_2 and both states of D_2O–SO_2 yield similar values as shown in Tables VI and VII. The larger uncertainties for the deuterat-

TABLE VI. Molecular constants of H_2O–SO_2 and D_2O–SO_2 (MHz).

Parameter	H_2O–SO_2 A_1 state	H_2O–SO_2 A_2 state	D_2O–SO_2 A_1 state	D_2O–SO_2 A_2 state
A	8763.071(3)[a]	8734.268(4)	8532.736(6)	8527.977(7)
B	3819.655(2)	3821.281(2)	3478.908(3)	3479.025(3)
C	2900.899(2)	2900.837(2)	2689.979(3)	2689.900(3)
δ_J	0.004 00(2)	0.004 05(2)	0.003 32(3)	0.003 23(4)
δ_K	0.161 9(8)	0.161 7(6)	0.134 1(10)	0.137 0(12)
Δ_{JK}	0.265 0(2)	0.265 4(1)	0.215 7(3)	0.215 1(3)
Δ_J	0.016 69(4)	0.016 70(4)	0.014 56(5)	0.014 57(6)
Δ_K	− 0.263 0(6)	− 0.273 5(8)	− 0.212 2(13)	− 0.216 0(16)
μ_a (D)	1.984(2)	1.984(2)	1.909(5)	1.902(10)
μ_c (D)	0.488(4)	0.470(5)	0.43(3)	0.49(4)

[a] One standard deviation uncertainties are given in parentheses and refer to the last digit(s) shown.

TABLE VII. Molecular constants of H_2O–$^{34}SO_2$ and HDO–SO_2 (MHz).

	H_2O–$^{34}SO_2$		HDO–SO_2
Parameter	A_1 state	A_2 state	Lower freq. state
A	8724.63(13)[a]	8695.91(33)	8641.6(34)
B	3793.630(1)	3795.237(3)	3636.70(9)
C	2890.211(1)	2890.161(3)	2795.69(8)
δ_J	0.004[b]	0.004[b]	0.003 66[c]
δ_K	0.161[b]	0.161[b]	−0.60(5)
Δ_{JK}	0.2606(14)	0.2605(35)	0.643(4)
Δ_J	0.016 62(7)	0.016 42(19)	0.0125(8)
Δ_K	−0.263[b]	−0.274[b]	−0.240[c]
μ_a (D)	...	...	1.92(2)
μ_c (D)	...	...	0.44(3)

[a] One standard deviation uncertainties refer to the last digit(s) shown.
[b] Parameter fixed at the value for H_2O–SO_2.
[c] Parameter fixed at the average of the values for H_2O and D_2O species.

ed species result from a smaller number of measurements, partially resolved deuterium hyperfine structure, and possibly larger errors in the computed Stark coefficients due to uncertainties in energy-level positions of HDO–SO_2. The similarity in values for the three isotopic species clearly indicates that no significant structural change occurs between the protonated and deuterated forms.

IV. STRUCTURAL ANALYSIS

The large second moment of inertia, $P_{cc} = \frac{1}{2}(I_a + I_b - I_c) = 7.88$ uÅ^2, clearly indicates that the complex is not planar and that at least one heavy atom is out of the plane of the other heavy atoms. Our initial structural assumptions were guided by prior work on H_2S–SO_2 (Ref. 13) and work in progress in our laboratory on H_2O–O_3.[14] For both of these complexes the H_2O and H_2S units lie above the plane of O_3 and SO_2, respectively. In the ozone complex the protons are located in the a,c plane, while for the SO_2 complex the protons are symmetrically displaced about this plane and closest to the oxygen atoms of SO_2 with a point group C_s for both complexes.

Since the μ_b moment was found to be zero, we assumed an a,c plane of symmetry. Also, the fact that $\Delta P_{bb} = -0.005$ uÅ^2 for ^{34}S substitution indicates that the sulfur atom lies in the a,c plane, and a similar examination of the change in moments for deuterium substitution shows that the deuterium atoms are located symmetrically out of the a,c plane. The moments of inertia of three isotopic species were fit to three parameters: $R_{c.m.}$, the center-of-mass separation; θ_1, the angle between $R_{c.m.}$ and the C_2 axis of SO_2; and θ_2, the angle between $R_{c.m.}$ and the C_2 axis of H_2O as shown in Fig. 1. The geometry of the monomer units was fixed at the values shown in Table VIII. A least-squares fit of the three moments of inertia for the H_2O, D_2O, and ^{34}S species resulted in the structural parameters listed in Table VIII. Two fits, labeled **a** and **b**, are given since the isotopic species studied do not allow a unique value for θ_1 to be determined, with the two values obtained being supplementary angles. Although the HDO species was not included in these fits, the calculated and observed rotational constants shown in Table IX are in good agreement. The observed dipole moment components compared with values derived from a simple vector sum of the monomer dipole moments,[16] $\mu_b(H_2O) = 1.855$ D and $\mu_b(SO_2) = 1.634$ D, as shown in Table IX, show much better agreement for fit-**a** structure than for the fit-**b** results, which strongly suggests that the correct structure is that from fit **a**.

In a further attempt to resolve the ambiguity in the θ_1 angle, we carried out a calculation of the ^{34}S substitution coordinates by the Kraitchman method.[17] According to Kraitchman's equations, the a-coordinate of the atom which is isotopically substituted is given by the following expression:

$$a_s = \left[\frac{\Delta P_{aa}}{\mu}\left(1+\frac{\Delta P_{bb}}{P_{bb}-P_{aa}}\right)\left(1+\frac{\Delta P_{cc}}{P_{cc}-P_{aa}}\right)\right]^{1/2}, \quad (1)$$

where P_{aa}, P_{bb} and P_{cc} are the principal second moments of the parent molecule and

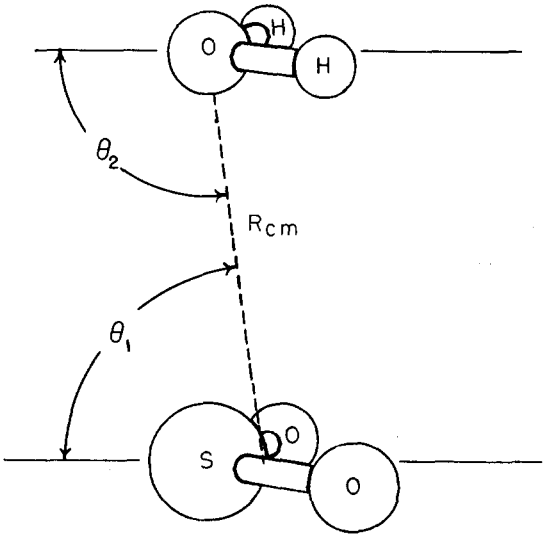

FIG. 1. Structural parameters employed in the analysis, the center-of-mass distance, and angles between $R_{c.m.}$ and the C_2 axes, are shown.

TABLE VIII. Molecular structure of H_2O–SO_2 and H_2S–SO_2.

Monomer geometry[a]	R_{XO}	θ_{XOX}
H_2O	0.958 Å	104.5°
SO_2	1.431 Å	119.3°
H_2S	1.336 Å	92.1°
H_2O–SO_2 fit parameters	Fit **a**	Fit **b**
$R_{c.m.}$	2.962(5) Å	2.959(10) Å
θ_1	69.7°(10)	108.8°(21)
θ_2	66.3°(14)	63.2°(31)
σ (uÅ^2)[b]	0.15	0.25
Derived values for H_2O–SO_2	Fit **a**	Fit **b**
$R_{O\text{-}S}$	2.824(16) Å	3.059(16) Å
$R_{H\text{-}O}$	3.334(15) Å	3.116(29) Å
ϕ_p[c]	134°(2)	98°(4)
H_2S–SO_2 fit parameters	Fit **a**	Fit **b**
$R_{c.m.}$	3.534(3) Å	3.534(4) Å
θ_1	81.0°(13)	98.3°(16)
θ_2	123.2°(11)	123.5°(14)
σ (uÅ^2)[b]	0.13	0.17
Derived values for H_2S–SO_2	Fit **a**	Fit **b**
$R_{S\text{-}S}$	3.520(9) Å	3.629(11) Å
$R_{H\text{-}O}$	3.145(18) Å	3.034(21) Å
ϕ_p[c]	66°(2)	48°(3)

[a] From Ref. 15.
[b] Standard derivation of the fit.
[c] Angle between monomer planes, 90° is the parallel configuration and 0° has the H's directed toward SO_2.

$$\mu = M_p \Delta m/(M_p + \Delta m), \tag{2}$$

for which M_p is the mass of the parent molecule and Δm is the change in mass upon substitution. The change in second moments is defined as

$$\Delta P_{xx} = P'_{xx} - P_{xx}, \tag{3}$$

for $x = a, b, c$ and P'_{xx} is the value for the isotopically substituted molecule. The b and c coordinate equations can be obtained from (1) by cyclic permutation of the subscripts. The results of this calculation are shown in Table X and compared with the S-atom coordinates of the two structure fits. It is clear from these values that the fit-**a** a coordinate is in good agreement with the substitution value, while fit **b** has a deviation of 0.2 Å for the a coordinate. The hydrogen-atom coordinates were also calculated by the double substitution method of Chutjian[18] and are presented in Table X. In this case comparison of the substitution coordinates with the fits does not provide substantial differences, although fit **a** appears to be in better agreement. The H–S distance calculated from these coordinates (see Table X) also agrees best with the value from fit **a**. Thus, fit-**a** structure, which also provides a smaller standard deviation as shown in Table VIII, gives the best overall agreement for the dipole moments and substitution coordinates. The preferred fit-**a** structure is shown in Fig. 2 along with the structure of H_2S–SO_2 obtained from a similar analysis.

TABLE IX. Comparison of the rotational constants for HDO–SO_2 and observed dipole moments with those derived from the structure fits.

	Obs.	Calc. fit **a**	Calc. fit **b**
Rotational Constants for HDO–SO_2			
A (MHz)	8641.4	8631.8	8634.3
B (MHz)	3636.71	3639.8	3644.0
C (MHz)	2795.68	2788.5	2790.8
Dipole moment components for H_2O–SO_2[a]			
μ_a (D)	1.984	1.31	0.31
μ_c (D)	0.49	0.19	0.10

[a] Absolute values compared.

TABLE X. Atomic coordinates for S and H from a Kraitchman analysis compared with those from the structure fits (in Å).[a]

	Atom coordinates		
	a	b	c
^{34}S substitution:	0.576	0	(−)0.366[b]
Structure fit **a**	0.518	0	−0.350
Structure fit **b**	0.775	0	−0.324
D_2 substitution:	(−)2.521[b]	±0.749	0.491
Structure fit **a**	−2.510	±0.757	0.531
Structure fit **b**	−2.554	±0.757	0.404
$R_{H\text{-}S}$ (substitution)	= 3.300 Å		
(fit **a**)	= 3.243 Å		
(fit **b**)	= 3.490 Å		

[a] Principal axes coordinates in center-of-mass frame.
[b] Only the magnitude, not the sign, is determined.

While comparing our structure results for H_2O–SO_2 with the H_2S–SO_2 complex, we noted an inconsistency in the reported structure of H_2S–SO_2. Bumgarner, Pauley, and Kukolich[13] carried out a Kraitchman analysis for the H atom in H_2S–SO_2 and obtained a coordinate $a_H = 1.79$ Å, while a value of 1.97 Å was obtained from their structure fit. This discrepancy led us to refit the structure of H_2S–SO_2 in the same manner as described above for the water complex in order to make structural comparisons. The present fit results

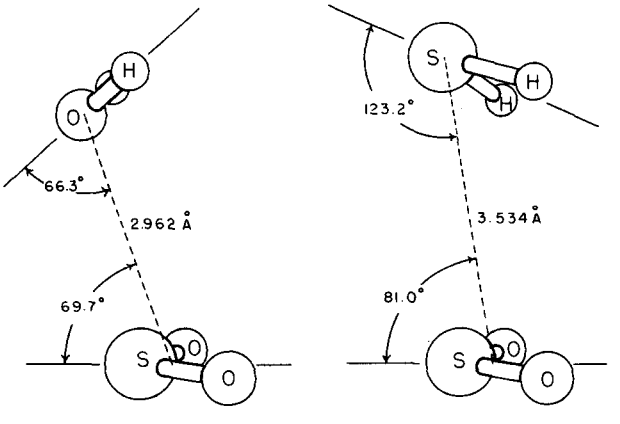

FIG. 2. Molecular structures of H_2O–SO_2 and H_2S–SO_2 from fit **a**. The a axis is nearly colinear with the dashed line joining the centers of mass and the b axis is perpendicular to the plane of the page.

are shown in Table VIII. In this fit the a coordinate for H is 1.82 Å, which agrees much better with the substitution value of 1.79 Å. The new structural parameters deviate significantly from the earlier results, especially in the angles. For comparison with the angular parameters reported previously, the supplementary angles $\theta = 180°-\theta_1 = 81.7°(16)$ and $\phi = 180°-\theta_2 = 56.5°(14)$ obtained from the present fit-**b** analysis should be compared with $\theta = 69°(4)$ and $\phi = 67°(9)$ reported by Bumgarner, Pauley, and Kukolich.[13] The source of these discrepancies may arise from fitting the rotational constants rather than the moments of inertia in the original analysis. In the present analysis, we find no compelling arguments to favor fit **a** over fit **b**. However, the consistency in θ_2 values for both fits indicates that the protons are directed toward the oxygen atoms of SO_2, although the H–O distance is larger than the van der Waals contact distance by 0.3–0.4 Å in both fits. The most striking difference in the structures of the H_2O and H_2S complexes is the orientation of the monomer planes, which is indicated by ϕ_p in Table VIII. These angles differ by 68° and 86° for fit **a** of H_2O–SO_2 and fits **a** and **b**, respectively, for H_2S–SO_2.

V. DISCUSSION

While one might expect to find similar structures for the three complexes, H_2O–O_3, H_2O–SO_2, and H_2S–SO_2, substantial differences are found in the positions of the hydrogen atoms. In the H_2O–SO_2 and H_2S–SO_2 complexes the hydrogens are located at 90° to the a,c plane (see Fig. 2), while in the H_2O–O_3 complex both hydrogens lie in the a,c-plane. The distances between the centers of mass of the monomer units, H_2O/SO_2 and H_2O/O_3, are also unusual in that they are nearly identical, i.e. $R_{c.m.} = 2.962$ Å for H_2O–SO_2 and $R_{c.m.} = 2.958$ Å for H_2O–O_3. In addition, the S–O distance in H_2O–SO_2 (2.824 Å) is about 0.4 Å shorter than the sum of the classical van der Waals radii, assuming values of 1.5 Å for oxygen and 1.85 Å for sulfur. This short bonding distance could be a result of a difference in effective van der Waals radii for divalent sulfur in species like H_2S compared with quadravalent S in SO_2. Perhaps a better view of the binding is that the more electropositive sulfur in SO_2, i.e., stronger Lewis acid, causes a stronger binding with water than does the central oxygen of ozone. If the van der Waals interaction is strongest for H_2O–SO_2, one would expect to find a substantially larger van der Waals bond-stretching force constant, k_s, and vibrational frequency, ω_s, for this species. Assuming that the van der Waals stretching mode is the major contribution to Δ_J, the pseudodiatomic model can be used to estimate the force constant and vibrational frequency from the equations given by Millen.[19] The estimates of these quantities are shown in Table XI and compared to three related complexes. The force constant and vibrational frequency for H_2O–SO_2 are significantly larger than for the O_3–H_2O and H_2S–SO_2 complexes and about equal to those of H_2O–CO_2 for which the C–O distance is also shorter than the sum of van der Waals radii by about 0.3 Å.

In contrast to the non-hydrogen-bonded structures of H_2O–SO_2 and H_2S–SO_2, complexes of SO_2 with the strong acids, HCl and HF, are clearly planar and hydrogen bonded[20] with an oxygen-to-hydrogen distance of about 2.0 Å. On the other hand, the complex of SO_2 with the weaker acid, HCN, is nonplanar and antihydrogen bonded[21] with a structural configuration similar to that of the H_2O–SO_2 complex. Goodwin and Legon[21] noted that a similar change from a hydrogen-bonded structure to an antihydrogen-bonded structure also occurs in the series CO_2–HX, where X = F, Cl, and CN. The CO_2 complexes with HF and HCl are linear,[22,23] but the HCN complex is T shaped with the N atom directed toward the C atom.[24] The antihydrogen bonding of the HCN, H_2O, and H_2S species with SO_2 is also paralleled in the CO_2 series since the heavy-atom configuration of the H_2O–CO_2 (Ref. 25) and H_2S–CO_2 (Ref. 26) complexes is T shaped with the hydrogen atoms directed away from CO_2.

TABLE XI. Comparison of van der Waals stretching force constants and vibrational frequency estimates.

H_2X–YO_2	ω_s (cm^{-1})	k_s (mdyn/Å)
H_2O–SO_2	80.1	0.053
D_2O–CO_2 [a]	80.2	0.052
H_2O–O_3 [b]	70.3	0.038
H_2S–SO_2 [c]	57.0	0.043

[a] Derived from data in Ref. 25.
[b] Derived from data in Ref. 14.
[c] Derived from data in Ref. 13.

The only prior spectroscopic study of the H_2O–SO_2 complex is an infrared matrix isolation study.[27] The general structural conclusions of Schriver, Schriver, and Perchard.[27] are consistent with the present results. They find that the bands assigned to H_2O in the complex are close to those of the proton acceptor molecule in $(H_2O)_2$, which suggests that the water oxygen atom is the electron donor and SO_2 is the acceptor. Their force-field analysis indicates that the two OH and SO oscillators are equivalent and both subunits maintain their local C_{2v} symmetry as concluded in our analysis. In addition to the 1:1 complex of water and SO_2, they also report evidence of the 1:2 and 2:1 complexes at higher concentrations of SO_2 or H_2O, respectively. While we made no effort to produce these trimers in our studies, one strong unassigned doublet transition was observed at 13 876.195 MHz and 13 876.375 MHz and required a higher concentration of water than did the 1:1 complex. Further searches will be necessary to identify the molecular source of these lines.

Further studies of other SO_x complexes are planned. Several systems which are important in SO_x chemistry are the O_3/SO_2, $O_3/H_2O/SO_2$, and H_2O/SO_3 mixtures. In addition to structural information on complexes produced, any chemical reaction in these mixtures will be important to quantify and relate to the mechanisms proposed in the formation of H_2SO_4.

[1] J. G. Calvert, A. Lazrus, G. L. Kok, B. G. Heikes, J. G. Walega, J. Lind, and C. A. Cantrell, Nature (London) **317**, 27 (1985).
[2] W. L. Chameides, In *Acid Deposition, Causes and Effects, A State Assessment Model*, edited by A. S. Green and W. H. Smith (Government Institute Inc., Rockville, MD, 1983), pp. 11–22.
[3] W. L. Chameides, J. Geophys. Res. **89**, 4739 (1984).
[4] L. Granat, Tellus **24**, 550 (1972).

[5]F. J. Lovas and R. D. Suenram, J. Chem. Phys. **87**, 2010 (1987).
[6]F. J. Lovas, R. D. Suenram, G. T. Fraser, C. W. Gillies, and J. Zozom, J. Chem. Phys. **88**, 722 (1988).
[7]L. H. Coudert, F. J. Lovas, R. D. Suenram, and J. T. Hougen, J. Chem. Phys. **87**, 6290 (1987).
[8]D. D. Nelson, Jr., G. T. Fraser, and W. Klemperer, J. Chem. Phys. **83**, 945 (1985).
[9]R. L. DeLeon, A. Yokozek, and J. S. Muenter, J. Chem. Phys. **73**, 2044 (1980).
[10]L. H. Coudert, F. J. Lovas, and K. Matsumura (in preparation).
[11]J. K. G. Watson, in *Vibrational Spectra and Structure*, edited by J. R. Durig (Elsevier, Amsterdam, 1977), Vol. 6, p. 1.
[12]L. H. Coudert and J. T. Hougen, J. Mol. Spectrosc. **130**, 86 (1988).
[13]R. E. Bumgarner, D. J. Pauley, and S. G. Kukolich, J. Chem. Phys. **87**, 3749 (1987).
[14]J. Z. Gillies, C. W. Gillies, R. D. Suenram, F. J. Lovas, T. Schmidt, and D. Cremer (in preparation).
[15]M. D. Harmony, V. W. Laurie, R. L. Kuczkowski, R. H. Schwendeman, D. A. Ramsay, F. J. Lovas, W. J. Lafferty, and A. G. Maki, J. Phys. Chem. Ref. Data **8**, 619 (1979).
[16]F. J. Lovas, J. Phys. Chem. Ref. Data **7**, 1445 (1978).
[17]J. Kraitchman, Am. J. Phys. **21**, 17 (1953).
[18]A. Chutjian, J. Mol. Spectrosc. **14**, 361 (1964).
[19]D. J. Millen, Can. J. Chem. **63**, 1477 (1985).
[20]A. J. Fillery-Travis and A. C. Legon Chem. Phys. Lett. **123**, 4 (1986).
[21]E. J. Goodwin and A. C. Legon, J. Chem. Phys. **85**, 6828 (1986).
[22]F. A. Baiocchi, T. A. Dixon, C. H. Joyner, and W. Klemperer, J. Chem. Phys. **74**, 6544 (1981).
[23]R. S. Altman, M. D, Marshall, and W. Klemperer, J. Chem. **77**, 4344 (1982).
[24]K. R. Leopold, G. T. Fraser, and W. Klemperer, J. Chem. Phys. **80**, 1039 (1984).
[25]K. I. Peterson and W. Klemperer, J. Chem. Phys. **80**, 2439 (1984).
[26]J. K. Rice, L. H. Coudert, K. Matsumura, R. D. Suenram, F. J. Lovas, W. Stahl, D. J. Pauley, and S. G. Kukolich (in preparation).
[27]A. Schriver, L. Schriver, and J. P. Perchard, J. Mol. Spectrosc. **127**, 125 (1988).